International Journal of Research in Engineering and Science (IJRES)
ISSN (Online): 2320-9364, ISSN (Print): 2320-9356
www.ijres.org Volume 2 Issue 9 ǁ September. 2014 ǁ PP.27-34

Study of electronic transport mechanism in carbon nanobuds (CNBs) using first-principles approach

Mudassir M. Husain*, Maneesh Kumar
Physics Section, Department of Applied Sciences and Humanities
Faculty of Engineering and Technology, Jamia Millia Islamia (a Central University)
New Delhi-110025 INDIA

Abstract : *In the present work we have investigated the electronic transport properties of fullerene functionalized single wall carbon nanotube (14,0) i.e. the carbon nanobuds (CNBs) with two different configurations using the first-principles density functional-based non-equilibrium Green function (NEGF) method. Our findings show that the localized states developed in the vicinity of bud region cause strong back-scattering and reduce the electron transmission significantly in the entire energy region. The I-V characteristics of the pristine CNT(14,0) show that it is semiconducting in nature with a threshold voltage 0.55 V. Upon fullerene functionalization of CNT (formation of small neck carbon nanobud) the threshold voltage changes to 0.60V. However on functionalization with long neck (6,0), no noticeable change in threshold voltages is observed. It has been further ascertained from I-V characteristic plots that zigzag nanotubes upon nanobud formation do not change their semiconducting nature. CNBs are promising candidates for nano electronics as they can enhance the cold field emission due to their charge distribution profile which extends from tube to the bud region.*

Keywords: *Carbon nanobuds (CNBs), Non-equilibrium Green function (NEGF), (14,0) SWCNT, Electrochemical potential, Transmission probability, I-V characteristics.*

I. Introduction

The discovery of fullerene [1] and carbon nanotube [2] played crucial role in the advancement of nanoscience and nanotechnology [3]. A carbon nanotube is not so reactive, on the other hand fullerene [4,5] due to its chemical properties, enables it to react with other compounds. Recent experimental studies have shown that these two carbon nanostructures can actually be engineered to form single hybrid carbon nanostructures. These hybrid nanostructures commonly known as nanobuds show special properties which can be utilized in designing nano devices in electronics. Smith et al. [6] experimentally functionalized nanotubes by filling them with C_{60}. According to them C_{60} enters nanotube through defects and forms the so called hybrid nanostructure nanopeapod, which can be utilized in fabricating molecular devices. Nanopeopad hybrid structures has been fabricated and reported by other groups [7-9] also. Nasibulin et al. [10, 11] synthesized novel hybrid material that combines fullerenes and SWCNTs into a single structure in which the fullerenes are covalently bonded to the outer surface of the nanotubes. According to them following are the two ways in which these hybrid structures form stable structures:

i) sp^3 hybridized structures formed through the chemisorption of perfect molecules C_{60} on SWNTs via [2+2] cycloaddition and [4+4] cycloaddition; in the former case a perfect structure of fullerene joins the nanotube with two C-C bond, while in the later it joins with four C-C bonds.
ii) sp^2 hybridized structures involves imperfect fullerene, covalently bonded to defective SWNTs. Such bonded structures are reminiscent of bud branch with a neck connecting the fullerene SWNT.

These fullerene functionalized SWCNTs are termed as nanobuds (CNBs). Due to high electrophilicity and curvature of fullerene moiety a carbon nanobud exhibits higher reactivity as compared to plane nanotube. The combined fullerenes in the carbon nanotubes modulate the electronic structures of the system [12], this modulated electronic structure gives rise to extraordinary observed properties e.g high current density and high cold electron field emission, which can be exploited in future nano devices. Theoretical insight into electronic structure of CNBs is essential before considering them for device applications. The electronic properties of CNBs in different configuration have been studied theoretically as well as experimentally by a number of groups [12-16] earlier. As electronic transport properties are crucial for determining how well the device will work and it has significance for device fabrication, we have investigated the electronic transport i.e transmission spectrum and I-V plots of above mentioned type (ii) sp^2 hybridized CNBs theoretically. A combination of first-

principles density functional theory (DFT) and non-equilibrium Green's function method has been used here for calculating the electronic transport properties of the system under consideration.

II. Model and computational method

As mentioned above fullerens can attach to SWCNTs to form carbon nanobuds (CNBs) via two ways [10,11] mentioned above. In the first case a perfect fullerene combines with SWCNT through sp^3 hybridization and in second case an imperfect or defective fullerene combines the SWCNT by sp^2 hybridization and it seems to be a continuous part of the nano tube. Zhao et al. [17] calculated the electronic transport properties of sp^3 bonded CNBs, (2+2) cycloaddition using two different types of SWCNTs, an arm chair (5,5) metallic and a zigzag (10,0) semiconducting. Fürst et al. [18] considerd sp^2 hybridized CNBs using armchair (5,5) metallic SWCNT for calculating the transmission spectra. In this work we have considered CNBs of second type as used by Fürst et al. (sp^2) and extended it for underlying semiconducting SWCNTs i.e. zigzag (14,0) instead of metallic . Moreover we have calculated the I-V characterstic curve of the CNBs. Fig. 1 shows the geometry of the CNBs we have investigated in this work and the device setup for calculating transmission and I-V characterstics. The SWCNT (10,0) and the CNBs are placed between two electrodes which serve as source (S) and drain (D); the system acts as channel (C) through which current flows on applying potential difference (V). Our calculations are based on a NEGF formalism coupled to Density functional theory (DFT) implemented in Atomix toolkit (ATK) program [19-21]. The electron transport in the nanosystems is considered in the form of ballistic transport, where the electrons in the channel (molecular junction) move straight through without suffering collisions (hence no mean free path). The ballistic electron transport calculations were performed using nonequlibrium Green's function (NEGF) formalism [22-25] and density functional theory [26-27]. In NEGF theory the transmission function T(E,V) of the system is a sum of transmission probabilities of all channels available at energy E under external bias voltage [22]

$$\mathrm{T(E,V)} = \mathrm{T_r}[\Gamma_\mathrm{L}(\mathrm{V})\mathrm{G^R(E,V)}\Gamma_\mathrm{R}(\mathrm{V})\mathrm{G^A(E,V)}]$$

where $\mathrm{G^{RA}}$ is the retarded and advanced Green's function, $\Gamma_{\mathrm{L,R}}$ are the imaginary parts of the left and right self-energies respectively. The I-V characterstics of the device can computed by invoking the Landauer-Büttiker [28,29] formalism, which relates the linear response conductance to the transmission probability T as

$$\mathrm{I(V)} = \frac{2\mathrm{e}}{\mathrm{h}} \int_{\mu_1}^{\mu_2} \mathrm{dE\ T(E,V)\ [f(E-\mu_L) - f(E-\mu_R)]}$$

where e, h have their usual meaning and μ_L , μ_R are the electrochemical chemical potentials of source and drain electrode; f is the Fermi-Dirac distribution function. When a bias voltage is applied between the contacts i.e. source (S) and drain (D), the current flows through the channel's (here nanotube (14,0), nanobuds CNB-0 and CNB-6) discrete energy levels which lies in the window between μ_L and μ_R. The bias voltage is symmetrically distributed. We have assumed zero temperature conductance and neglected noncoherent charge transport processes that could couple different transverse modes. While computing I-V characterstics, we have adopted the approximation of employing the zero-bias transmission $\mathrm{T(E,V=0)}$ to compute the current I at finite bias V. The current is determined by integrating the area under the transmission curve within the bias window $(\mu_\mathrm{L}, \mu_\mathrm{R})$. Initially geometries of isolated systems have been relaxed using Brenner empirical potential [30] keeping maximum force $0.05\ \mathrm{eV/Å}$, maximum stress $0.05\ \mathrm{eV/Å^3}$. Fürst et al. [18] verified that relaxing the structures using Brenner empirical potential leads to insignificant changes in the transport properties as compared to a high quality density functional theory (DFT). For transport calculations the optimized structures are placed between source and drain extending the SWCNTs to left and right infinities to form the electrodes and molecular junctions. The electronic transport properties of the molecular junctions are calculated by a fully self-consistent NEGF formalism combined with first-principles DFT implemented ATK program [19]. The exchange-correlation potential is described by LDA; core electrons are modelled with Troullier-Martins non-local pseudopotential [31]. The electrode calculations are performed under periodic boundary conditions. Brilloun zone has been sampled with $1 \times 1 \times 100$ points within the Monkhorst-Pack k-point sampling method [32] in case of our one-dimensional molecular junction. The self-consistent calculations are performed with a mixing rate set to 0.01 and the convergent criterion for total energy is 10^{-5} eV. A single-ς basis set is used with 150 Ry mesh cut off.

III. Results and Discussion

For denoting carbon nanobud CNBs we have used the notation CNB-n, where n denotes the number of unit cell of (6,0) SWNT in the neck region. Thus CNB-0 denotes cabon nanobud without a neck (a fullerene dome on CNT) and CNB-6 denotes the carbon nanobud with (6,0) neck with six unit cells in the neck region.

Fig.1 (a-c) shows the pristine (14,0) SWCNT, CNB-0 and CNB-6 with 392, 452 and 524 carbon atoms respectively. The desired physical quantity in transport calculations is the transmission function T(E). Its value at Fermi level E_F gives the zero-bias conductance. The current can be obtained by integrating over the bias dependent energy window. The calculated transmission functions T(E) under zero bias for CNB-0 and CNB-6 are shown in Fig. 2(a) and 3(a) respectively along with the parent pristine (14,0) SWCNT. A glance at both plots shows that there is drop in transmission on bud formation and appearance of peaks in transmission spectrum over the entire energy range as compared to the pristine SWNT which shows clear cut stepwise features. This decrease has been observed by Zhao et al. [17] sp^3 hybridized CNB55 and CNB100. The decrease in transmission in the present case may be attributed due i) the vacancies responsible for reducing the transmission [33-36] predominantly when they are adjacent ii) Localized states in bud and neck region cause strong back scattering. It is apparent from these transmission plots upon bud formation of these CNBs retain their semiconducting nature. Fig. 2(b) and 3(b) shows MPSH (Molecular Projected Selfconsistent Hamiltonian) plot of highest occupied molecular orbital (HOMO) and lowest unoccupied molecular orbital (LUMO) of CNB-0 and CND-6 respectively. It is obvious from from these MPSH that the charge is localized in bud region of LUMO and it is completely delocalized in HOMO. The localization of charge in LUMO is around the C_{60} moiety in CNB-0 and in neck region of CNB-6 (magnitude of concentration of charge in this region seems to be more). These localized states near bud region cause strong back scattering which results in drop of transmission [18]. The backscattering has important applications in nanoelectronics and makes CNBs excellent candidates for cold electron field emission, as electrons can be pumped to LUMO initially and then emitted to vacuum through the bud regions which act as potential emission sites [11,15]. As zero bias voltage gives limited insight into the electron transport mechanism; we have calculated the transmission spectrum of both the CNBs under investigation at five different bias voltages ranging from 0 to 2.0 V in a step of 0.5 V and the results are presented in Figs. 4,5. As can be seen from Figs. 2(a), 3(a) , 4 and 5 there is no transmission at 0 V and therefore no conduction. However as the bias voltage is increased the transmission increases and new peaks appear around the fermi level. There is no peak at zero bias however as the bias voltage is increased the width between electrochemical potentials $\Delta\mu = \mu_L - \mu_R$ increases and more number of peaks appears and the magnitude of transmission increases as the voltage is increased.

The electronic transport through the molecular junction gives rise to current. Fig. 6 shows the I-V characteristics of CNB-0 and CNB-6 along with the parent (14,0) SWNT. The voltage across these molecular junctions is varied from 0 to 1.6 V and the current is measured. The I-V characteristic plots are presented in Fig. 6 (a). The curve shows that the current increases after a certain minimum threshold value of voltage which shows semi conducting nature of the buds. The threshold value of voltage of CNB-6 is same as that of nanotube i.e. 0.55V however for CNB-0 it is 0.60V. Our observation shows that the semiconducting nature of the (14,0) SWCNT is preserved on bud formation.

IV. Conclusion

The electron transport properties i.e the transmission and I-V characteristics of sp^3 hybridized carbon nanobuds using zigzag and metallic SWCNs has been reported [17]. Also the transmission spectrum of sp^2 hybradized CNBs using armchair has been studied [18]. We have extended our studies so as to complete the investigation of sp^2 hybradized CNBs using semiconducting (14,0) CNTs and to study the electronic transport at different bias voltages. We have also studied I-V characteristic of this typs of CNBs for the first time. It is evident from I-V Characteristics the pristine (14,0) SWCNT which is semiconducting retains is semiconducting nature on CNB formation. As charge distribution can get localised in the bud region we conclude that these nanobuds can be used as active elements in nanoelectronics as cold electron field emitter.

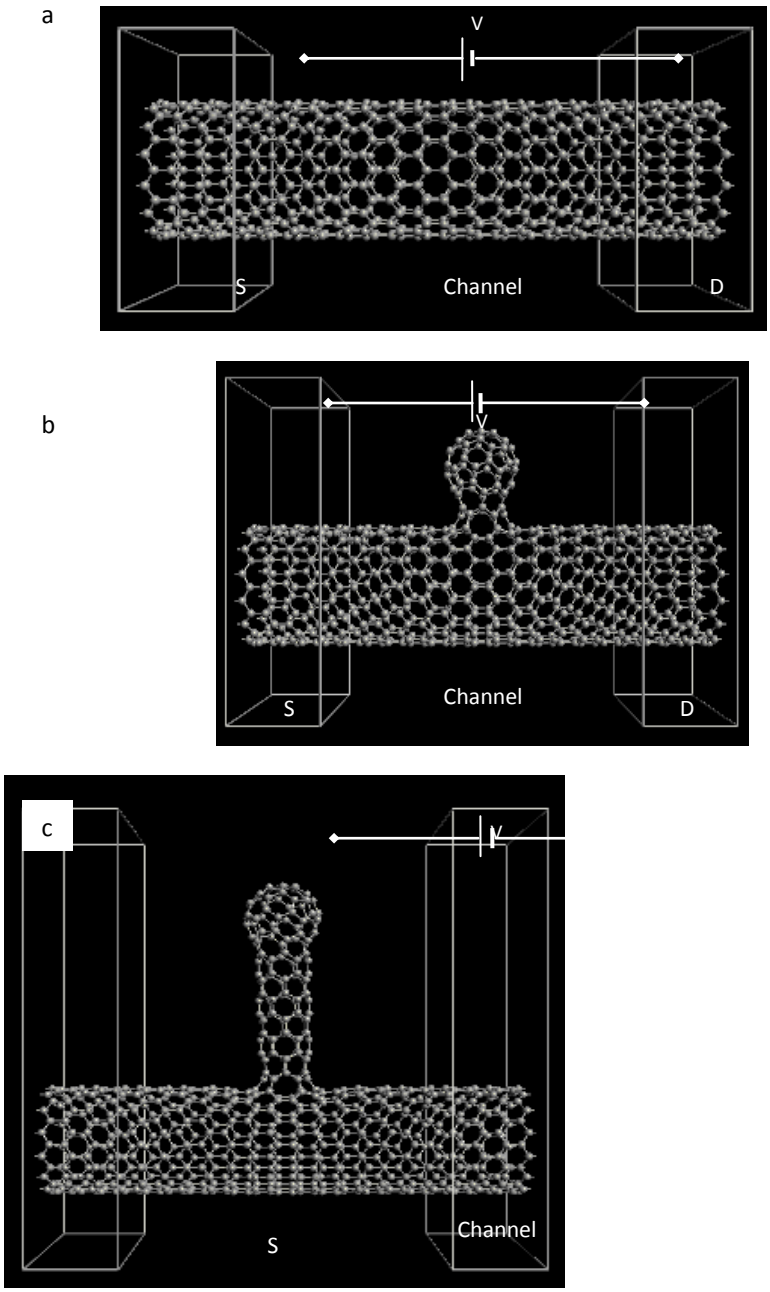

Fig.1. Device setup of optimized a) single-wall carbon nanotube: SWCNT (14,0) b) carbon nanobud: CNB-0 and c) carbon nanobud: CNB-6. The CNB consists of an imperfect C60 attached to CNT(14,0) single-wall nanotube (SWNT) via a neck region. The number of unit cells in neck region of a) CNB-0 is zero while in b) CNB-6 is six with (6,0) CNT neck (S: Source, D: Drain)

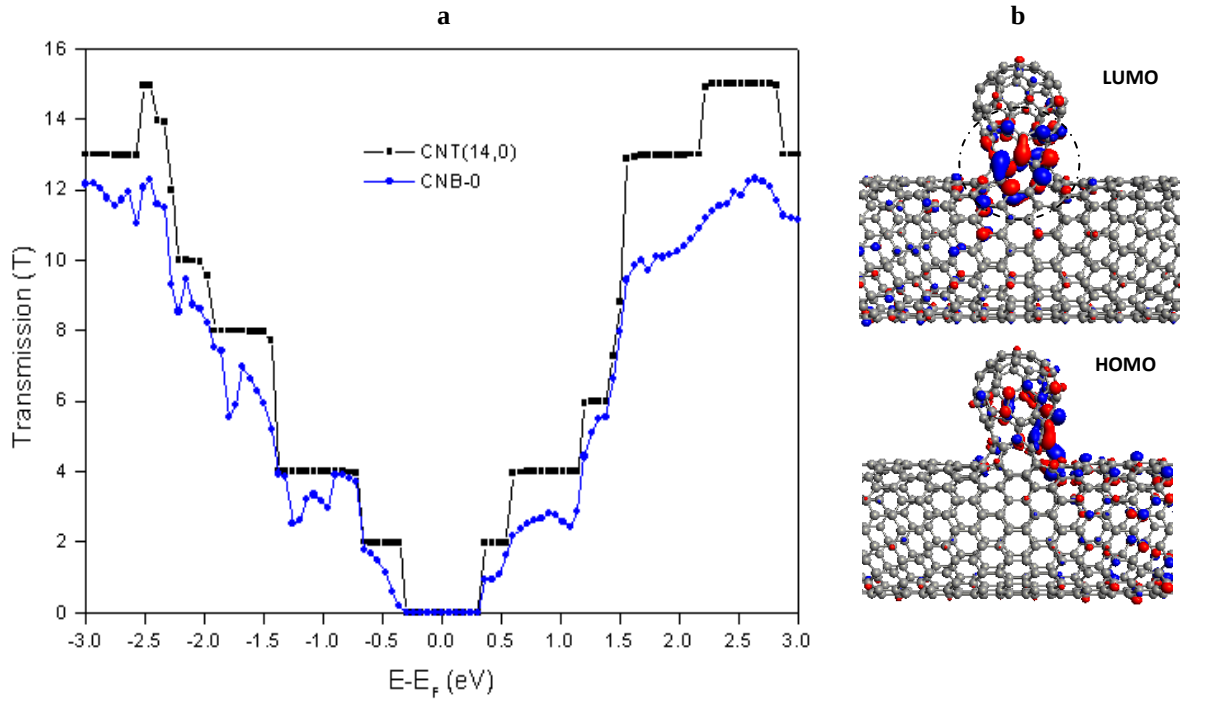

Fig. 2. a) Comparision of zero-bias transmission spectrum of carbon nanobud CNB-0 (short neck, shown in blue color online) and pristine (14,0) SWCNT (shown in black line). The transmission of CNT shows stepwise features while upon nanobud formation the peak appears. b) The molecular projected self-consistent Hamiltonian (MPSH) eigen states of the HOMO and LUMO of CNB-0.

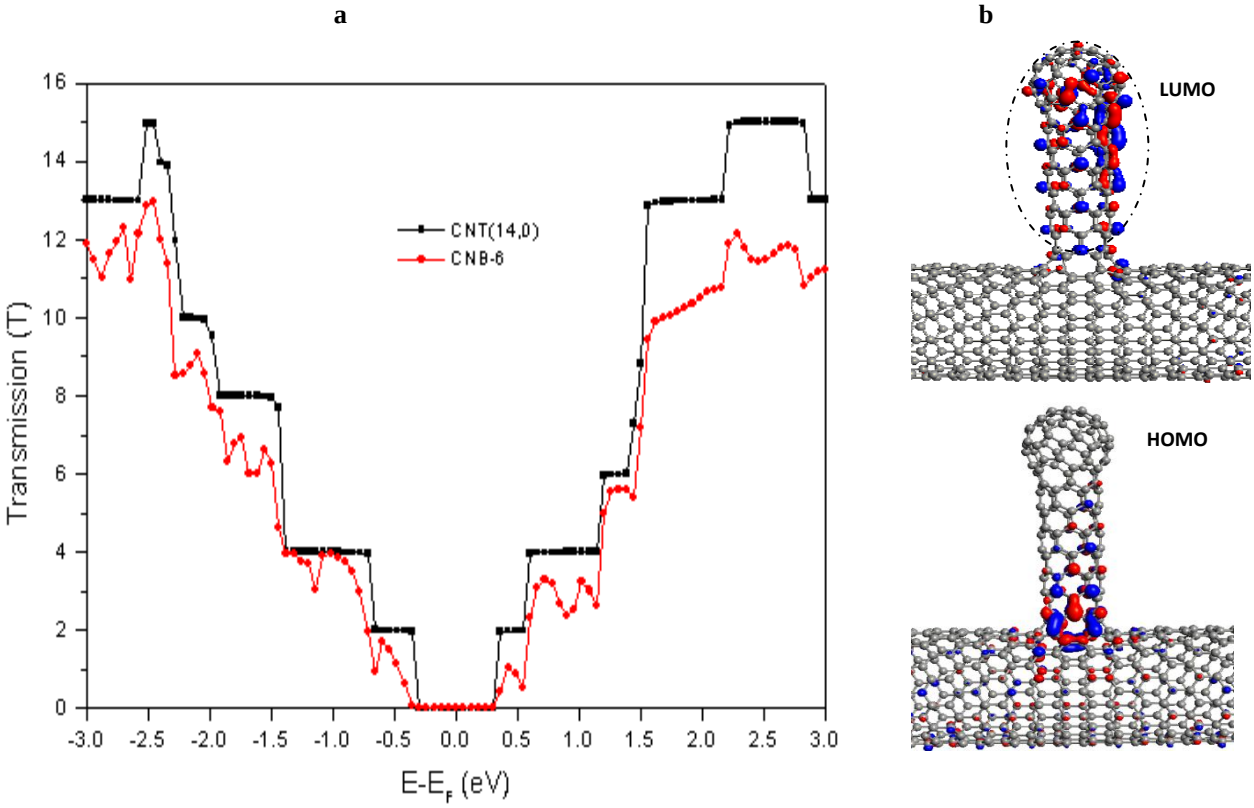

Fig. 3. Comparision of zero-bias transmission spectrum of carbon nanobud CNB-6 (long neck, shown in red color online) and pristine (14,0) SWCNT (shown in black line). The transmission of CNT shows stepwise features while upon nanobud formation the peak appears. b) The molecular projected self-consistent Hamiltonian (MPSH) eigen states of the HOMO and LUMO of CNB-6.

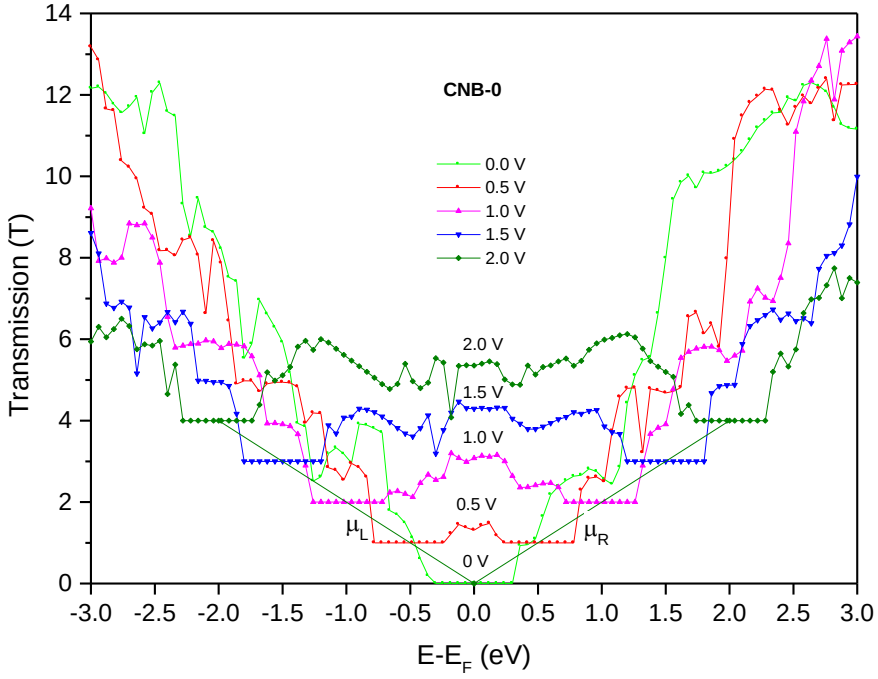

Fig. 4. Bias dependence of transmission spectrum of CNB-0 junction. The bias voltages applied are 0V (green), 0.5 V (red), 1.0V (magenta), 1.5 V (blue), 2.0 (olive); μ_L and μ_R are the chemical potentials of source (S) and drain (D) electrodes respectively.

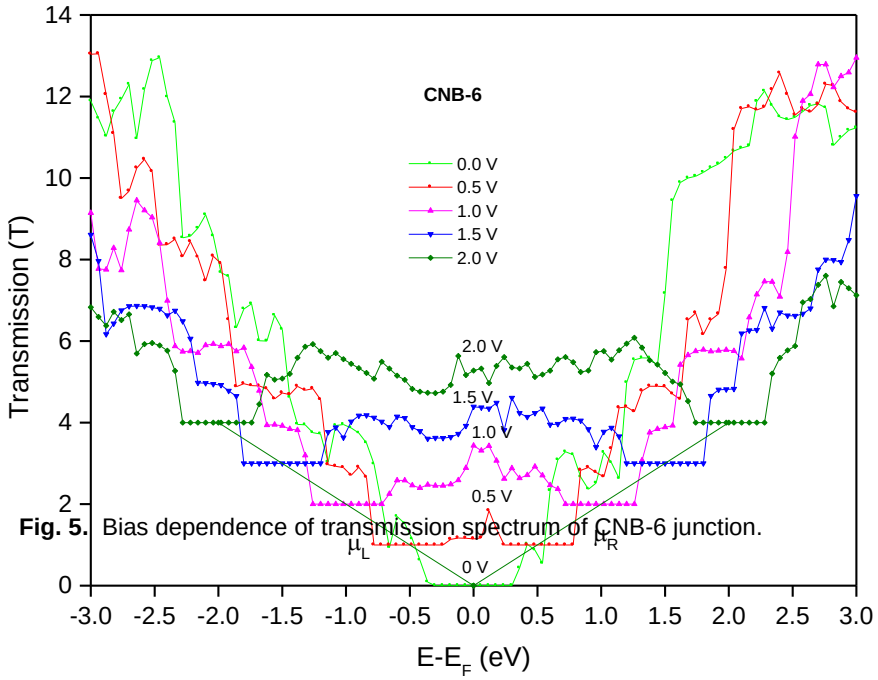

Fig. 5. Bias dependence of transmission spectrum of CNB-6 junction.

a

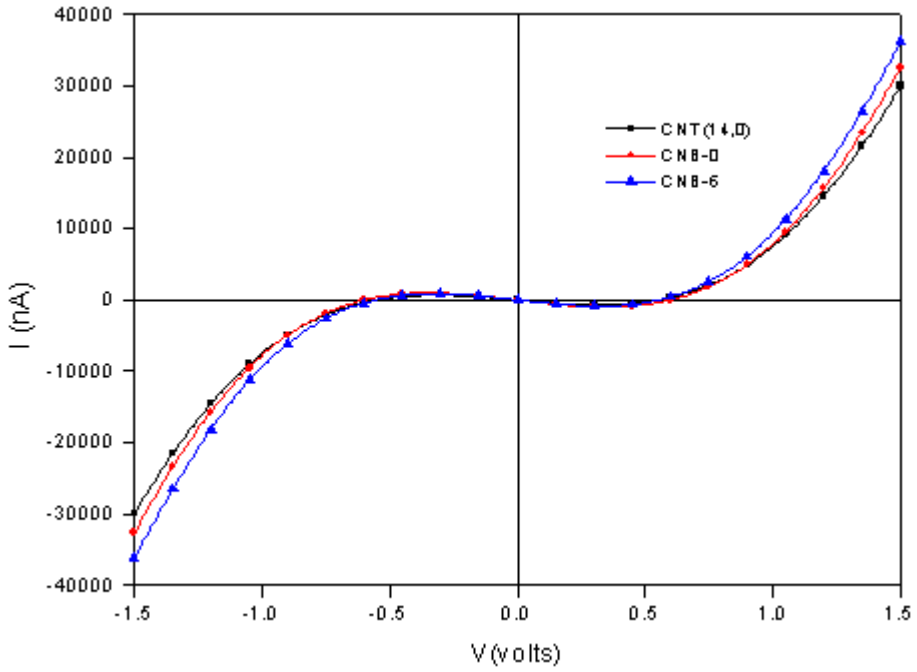

b

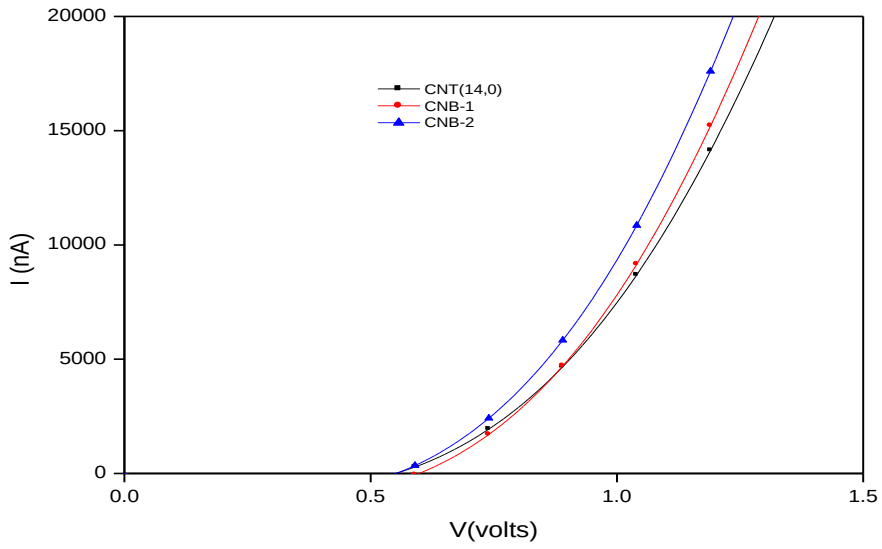

Fig. 6. A comparison of current-voltage (I-V) characterstics for SWCNT (14,0), CNB-0 and CNB-6. a) shows behaviour of curve from -1.5 to 1.5 V b) Forward biased

References

[1] H.W. Kroto, J.R Heath, S.C. O' Brien, R.F. Curl, R.E. Smalley, Nature 318 (1985) 162.
[2] S. Ijima, Nature 354 (1991) 56.
[3] M.S. Dresselhaus, G. Dresselhaus, P.C. Eklund, Acdemic Press; New York, (1996).
[4] R.C. Haddon, Science 261 (1993) 1545.
[5] F. Diederich, C. Thilgen, Science 271 (1996) 317.
[6] B.W. Smith, D. E.Luzzi, Chem. Phys. Lett. 321 (2000) 169.
[7] D.J. Hornbaker, S.J. Kahng, S.Mishra, B.W. Smith, A.T. Johnson, E.J. Mele, D.E.Luzzi, A.Yazdani, Science 295 (2002) 282.

[8] J. Lee, H. Kim, S. J. Kahng, G. Kim, Y. W. Son, J. Ihm, H. Kato, Z. W. Wang, T. Okazaki, H. Shinohara, Y. Kuk, Nature 415 (2002) 1005.
[9] F. Ding, Z. Xu, B.I. Yakobson, R.J.Young, I.A. Kinloch, S. Cui, L. Deng, P. Puech, M. Monthioux, Phys. Rev. B 82 (2010) 041403.
[10] A.G. Nasibulin, P.V. Pikhitsa, H. Jiang, D.P. Brown, A.V Krasheninnikov, A.S. Anismov, P.Queipo, A. Moisala, D. Gonzalez, G. Lienrsching, A. Hassanien, S.D. Shandakov, G. Lolli, D.E. Resasco, M. Choi, D. Tomanek, E.I. Kauppinen, Nat. Nanotechnol. 2 (2007) 156.
[11] A.G. Nasibulin, A.S. Anismov, P.V. Pikhitsa, H. Jiang, D.P. Brown, M. Choi, E.I. Kauppinen Chem. Phys. Lett. 446 (2007) 109.
[12] H. Y. He, B. C. Pan J. Phys. Chem. C 113 (2009) 20822.
[13] T. Menz, C-Y. Wang,S-Y Wang Phys. Rev. B 77 (2008) 033415.
[14] A. Seif, E.Zahedi, T.S. Ahmadi, Eur. Phys. J. B 82 (2011)147.
[15] X. Wu, X. C. Zeng, Am. Chem. Soc. Nano 2,7 (2008) 1459.
[16] M. He, E. Rikkinen, Z. Zhu, Y.Tian, A.S. Anisimov, H. Jiang, A.G. Nasibulin, E.I. Kauppinen, M Niemelä, A.O.I. Krause, J. Phys. Chem. C 114 (2010) 13540.
[17] P. Zhao, P.J. Wang, Z. Zhang, M.J. Ren, D. S. Liu, Physica B 405 (2010) 2097.
[18] J. A Fürst, J. Hashemi, T. Markussen, M. Brandbyge, A.P. Jauho, N. Nieminen, Phys. Rev. B 80 (2009) 035427.
[19] See http://www.quantumwise.com for "Atomistix Toolkit Version 12.2.2", Quantumwise a/s.
[20] J. Taylor, H. Guo, J. Wang, Phys. Rev. B 63 (2001) 245407.
[21] M. Brandbyge, J. L. Mozos, P. Ordejon, J. Taylor, K. Stokbro, Phys. Rev. B 65 (2002) 165401.
[22] S. Datta, Quantum Transport: Atom toTransistor, Cambridge University Press (2005)
[23] S. Datta, Superlattices Microstruct, 28, 253 (2000) 253.
[24] A. D. Carlo, M. Gheorghe, P. Lugi, M. Sternberg, G. Seifert, T. Frauenheim, Physica B 314 (2002) 86.
[25] H. Huag, A. Jauho, Quantum Kinetics in Transport and Optics of Semiconductors (Springer Verlag, 2008) Vol. 2.
[26] D. Porezag, T. Frauenheim, T. Köhler, G. Seifert, R. Kaschner, Phys. Rev. B 51 (1995) 12947.
[27] M. Elstner, D. Porezag, G. Jungnickel, J. Elsner, M. Haugk, T. Frauenheim, S. Suhai, G. Seifert, Phys. Rev. B 58 (1998) 7260.
[28] R. Landauer, Philos. Mag. 21 (1970) 863.
[29] M. Büttiker, Phys. Rev. Lett. 57 (1986) 1761.
[30] D. W. Brenner, Phys. Rev, B 42 (1990) 9458.
[31] N. Troullier, J. Martins, Phys. Rev. B 43 (1991) 1993.
[32] H.J. Monkhorst, J.D. Pack, Phys. Rev. B 13 (1976) 5188
[33] L. Chico, L. X. Benedict, S. G. Loui, M. L. Cohen, Phys. Rev. B 54 (1996) 2600.
[34] M. Igami, T. Nakanishi, T. Ando, J. Phys. Soc. Jpn 68 (1999) 3146.
[35] A. Hansson, M. Paulsson, S. Stafström, Phys. Rev. B 62 (2000) 7639.
[36] H.J. Choi, J. Ihm, S. G. Louie, M. L. Cohen, Phys. Rev. Lett. 84 (2000) 2917.